Available online at www.sciencedirect.com

ScienceDirect

Materials Today: Proceedings 2S (2015) S759 – S762

International Conference on Martensitic Transformations, ICOMAT-2014

NiTiCu transverse to axial strain ratio analysis during tension/compression tests

A. Fabregat-Sanjuan[a,]*, F. Ferrando[a], S. De la Flor[a]

[a]*Universitat Rovira i Virgili, Av. Països Catalans, 26, ETSEQ, Tarragona 43007, Spain*

Abstract

Tension-compression asymmetry in polycrystalline NiTiCu tubes was studied during elastic and transformation zone using strain gauges rosettes. Axial and transverse strain measurements from strain gauges were used to calculate a localized strain ratio through tensile and compression tests at different temperatures. The results show an asymmetric tension/compression behavior from stress-axial strain curves and from strain ratio-axial strain curves with a non constant strain ratio. Different temperatures tests also show similar values of strain ratio for martensite and austenite phases in the elastic zone.

Selection and Peer-review under responsibility of the chairs of the International Conference on Martensitic Transformations 2014.

Keywords: Strain ratio; Poisson; asymmetry; NiTiCu; tension; compression; strain gauge; rosette

---

1. Introduction

Tension-compression asymmetry in polycrystalline NiTiCu tubes was studied during elastic and transformation zone using strain gauges rosettes. Axial and transverse strain measurements from strain gauges were used to calculate a localized strain ratio through tensile and compression tests. This strain ratio is similar to Poisson's ratio, in that it represents the relationship between axial and transverse strain. However, while Poisson's ratio is of purely linear elastic strains, the strain ratio includes both elastic and inelastic effects such as strain accommodated by the phase transformation.

---

* Corresponding author. Tel.: +34-977-559-660; fax: +34-977-559-691.
E-mail address: albert.fabregats@urv.cat

Selection and Peer-review under responsibility of the chairs of the International Conference on Martensitic Transformations 2014.
doi:10.1016/j.matpr.2015.07.393

Strain ratio's measurements are critical for a better understanding and modeling of these materials. This data is largely lacking in the literature and there are typical modeling assumptions, which input strain ratios as constant values for transforming and elastically deforming NiTi based alloys. The strain ratio is quoted as 0.5 during phase transformation [1–3], and 0.3 is often used for non-transforming loadings. Recently, digital image correlation has been used to investigate this phenomenon [4]. At the same time, neutron diffraction studies and micromechanical simulations have calculated effective Poisson's ratios under loading using macroscopic elastic parameters [1,5]. The majority of the studies are based on pseudoelastic or superelastic alloys that have austenite phase (B2) at room temperature which transforms via a stress-induced transformation to detwinned martensite (B19') and recover upon unloading. However, there is a lack of studies of the strain ratio of shape memory effect alloys, which are useful because they are recovered via moderate temperature increases (actuator purposes). For this reason, this study has been done in a shape memory effect alloy that has twinned (self-accommodated) martensite phase (B19') at room temperature and deforms through stress induced transformation into detwinned martensite phase (B19').

2. Materials and methods

$Ti_{44.6}Ni_5Cu$ (%at.) tubes with a diameter of 10.25mm, wall thickness of 1 mm and length of 150 mm were used in this study. A heat treatment (HT) for shape-setting was carried out for 60 minutes at 450 ºC followed by water quenching, which assure fully martensitic phase at room temperature (M_f=33 ºC, M_s=41 ºC, A_s=53 ºC, A_f=59 ºC).

Tension/Compression tests were carried out in a Zwick 1445 tensile test machine with an adapted thermal chamber. To verify that local results from the strain gauge could be considered as a macroscopic behaviour, preliminary tests were done with strain gauges and a 50 mm length extensometer at the same time. The results from extensometer and strain gauges were comparable and the strain gauges use was validated. Fig. 1 shows the tubes used on the experiments. Tensile test specimens ends were modified to grip the tube on the clamps. Compression specimens were reduced to 75mm length to avoid buckling problems in high stress tests. Rosette gauges were adhered and connections and calibrations were done to ensure data acquisition. Data acquisition from strain gauges and load cell was done through a P3 Strain indicator and recorder from Vishay. All tests were done at a strain rate of 0.5 mm/min to ensure that the strain rate had no undue effect on the test.

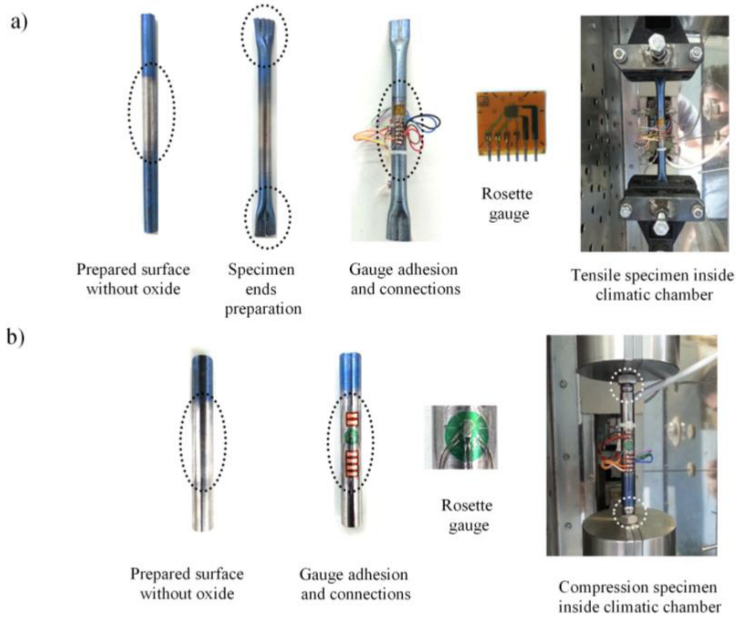

Fig. 1. (a) Tension test configuration; (b) Compression test configuration.

3. Results

3.1. Tension/compression asymmetry

Tension/compression asymmetry can be identified in Fig. 2. Under tension, a clear stress plateau occurs, while under compression, the material is quickly strain hardened and no clear stress-plateau can be observed. This shows that the deformation mechanisms are different for tension and compression. Other authors have also studied this tension/compression asymmetry. Liu et. al. [6] showed that under tension, two adjacent martensite plates containing twins become compound twin related to each other and, as a result, the interface between the two martensite variants have partially reoriented via migration of these interfaces when tensioned. Under compression, a high density of dislocations has been generated in both the martensite twin plates and the junction plane areas. The asymmetry can be also detected through the differences in the elastic moduli at room temperature (T<Mf). Tensile tests show a value around 35 GPa and compression tests show a higher value around 40 GPa. This difference can also be related to the crystallographic asymmetry of the martensitic phase transformation and textures due to drawing process along the longitudinal tube axis.

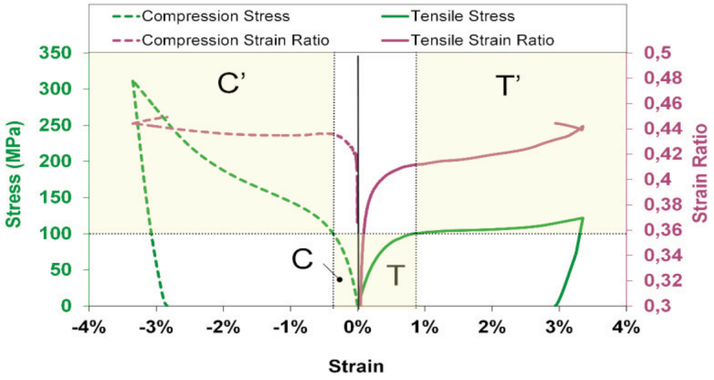

C' → Constant strain ratio value at compression:
Stress range: From 100 to 310 MPa
Strain range: From 0.3% to 3%
C → Variable strain ratio value at compression:
Stress range: From 0 to 100 MPa
Strain range: From 0 to 0.3%
T' → Constant strain ratio value at tension:
Stress range: From 100 to 120 MPa
Strain range: From 0.8% to 3%
T → Variable strain ratio value at tension:
Stress range: From 0 to 100 MPa
Strain range: From 0 to 0.8%

Fig. 2. Tension/compression asymmetry and strain ratio analysis at room temperature ($T<M_f$).

3.2. Strain ratio

Stacked strain gauges rosettes enable the measure of both axial and transverse strain on the same point. This is interesting because reduces error measurements derived from the effects of the strain localization and propagation on the stress-induced transformations in tension [4]. The localized strain ratio was calculated as the relation between the transverse and axial strain.

The localized strain ratio is shown as a function of the axial strain at room temperature in Fig. 2. The strain ratio increases in the elastic zone and remain quasi-stable once the transformation starts (100 MPa). For tensile tests the strain ratio value stabilizes at 0.41 once the transformation starts (0.8% of strain) and gradually increases until 0.44 at 3.3% of strain. For compression tests the strain ratio is more stable and gets a value around 0.44 from 0.3% of strain until 3.3% of strain. Others authors have found similar values such as Bewerse et. al [4] (0.4-0.45 for tension and 0.51 for compression), Qiu et. al. [1] (between 0.387 and 0.45), Heinen et. al. [7] (0.47) and Wagner et. al. [3] (0.36). However, most of the studies done are not totally comparable because the studies are done with NiTi alloys instead of the NiTiCu alloy and they also work with superelastic alloys which have austenite phase at room temperature.

To study the influence of the strain ratio's variation due to the austenite or martensite phase, several tests were done at different temperatures from a temperature below M_f to a temperature above A_f. The results from these tests are shown in Fig. 3. The stress level chosen was 40 MPa to have the strain ratio for twinned martensite and austenite because is under the critical stress (starting of detwinned martensite).

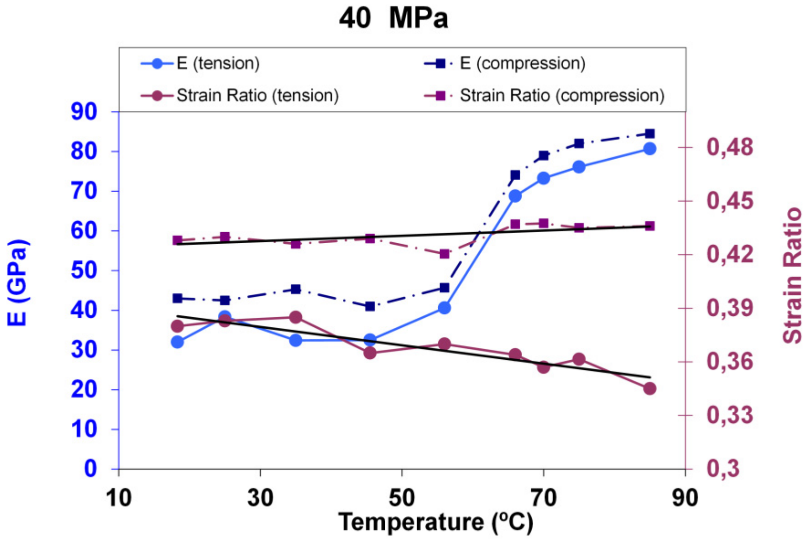

Fig. 3. Strain ratio and elastic moduli evolution with temperature.

Fig. 3 shows the evolution of the elastic moduli and strain ratio on tension and compression tests (40MPa) at different temperatures. The elastic modulus of compression tests is higher than the obtained on the tensile tests for all temperatures; it is coherent with the asymmetry analysis done in the previous section. Although strain ratio depends on the stress level, it is interesting to point out that if a particular stress level wants to be studied, the strain ratio's variations with temperature are small and a simplification with a constant value or a linear tendency can be chosen for modeling purposes. Fig. 3 shows that for a stress level of 40 MPa a strain ratio value of 0.43 can be chosen for compression tests and a value between 0.35-0.38 can be chosen for tensile tests.

4. Conclusions

- Rosette strain gauges can be used as an alternative method to analyze the transverse to axial strain ratio at both elastic and transformation zones.
- Transverse to axial strain ratio cannot be properly modeled with a constant value and has to be evaluated at different strain/stress levels. However, after the detwinning process starts there are only slight changes on the variation of the strain ratio and, if necessary, a simplification can be done with the following constant values: 0.41-0.44 for tension and 0.44 for compression.
- Transverse to axial strain ratio does not almost change with temperature for stress levels below critical stress and twinned (self-accommodated) martensite phase and austenite phase show similar values of strain ratio.

References

[1] S. Qiu, B. Clausen, S. a. Padula, R.D. Noebe, R. Vaidyanathan, Acta Mater. 59 (2011) 5055–5066.
[2] X. Gao, A. Stebner, D.W. Brown, L.C. Brinson, Acta Mater. 59 (2011) 5924–5937.
[3] M.F.-X. Wagner, W. Windl, Acta Mater. 56 (2008) 6232–6245.
[4] C. Bewerse, K.R. Gall, G.J. McFarland, P. Zhu, L.C. Brinson, Mater. Sci. Eng. A. 568 (2013) 134–142.
[5] A. P. Stebner, S.C. Vogel, R.D. Noebe, T. a. Sisneros, B. Clausen, D.W. Brown, et al., J. Mech. Phys. Solids. 61 (2013) 2302–2330.
[6] Y. Liu, Z. Xie, J. Van Humbeeck, L. Delaey, Acta Mater. 46 (1998) 4325–4338.
[7] R. Heinen, K. Hackl, W. Windl, M.F.-X. Wagner, Acta Mater. 57 (2009) 3856–3867.